

## Corrosion Behavior of a Motor-Driven Filter Pipeline in Seawater Using the Weight Loss Method: Effect of Temperature and Flow

M.C. Fatah<sup>1\*</sup>, A.R. Pratama<sup>2</sup>, A.W. Pramono<sup>3</sup>

<sup>1,2</sup>Mechanical Engineering Department, Faculty of Technology and Energy Business, Institut Teknologi PLN, Jl. Lkr. Luar Barat, Duri Kosambi, Jakarta 11750, Indonesia.

<sup>3</sup>Research Centre for Advanced Materials, National Research and Innovation Agency, Building 720, Science and Technology Park BJ Habibie, Serpong, South Tangerang 14314, Banten, Indonesia.

\*E-mail: Martin@itpln.ac.id

### ABSTRACT

Failure of a motor-driven filter pipeline was reported due to seawater-induced corrosion. The objective of this study was to investigate the corrosion behavior of the pipeline material in seawater under static and dynamic conditions at temperatures of 27, 40, 60, and 80°C using the weight-loss method. Surface characterization was performed using scanning electron microscopy coupled with energy-dispersive spectroscopy (SEM-EDS) and X-ray diffraction (XRD). At 80°C, both static and dynamic conditions exhibited corrosion rates approximately twice those observed at 27°C. SEM observations revealed the formation of a dense and adherent corrosion-product layer at 27°C. However, at 80°C, cleavage and cracking of the corrosion-product layer were observed, allowing corrosive species to diffuse more readily to the metal surface and thereby accelerating corrosion. XRD analysis confirmed that the corrosion products consisted primarily of Fe<sub>2</sub>O<sub>3</sub> (hematite) and Fe<sub>3</sub>O<sub>4</sub> (magnetite).

**Keywords:** Carbon steel, Sea water, SEM-EDS, Weight loss, XRD.

### ABSTRAK

Sebuah kegagalan pada pipa motor driven filter dilaporkan akibat air laut. Tujuan dari penelitian ini adalah untuk mempelajari korosi yang disebabkan oleh air laut pada pipa motor driven filter pada kondisi statis dan dinamis di suhu 27, 40, 60, dan 80°C menggunakan metode weight loss. Karakterisasi permukaan logam dilakukan menggunakan SEM-EDS dan XRD. Pada suhu 80°C, pada kondisi statis dan dinamis, terdapat kenaikan laju korosi sebanyak 2 kali lipat di bandingkan laju korosi pada suhu 27°C. Uji SEM menunjukkan terbentuknya film yang padat pada suhu 27°C. Akan tetapi, pada suhu 80°C, celah terbentuk pada permukaan film sehingga senyawa korosif berdifusi ke permukaan logam dan menyebabkan meningkatnya laju korosi. XRD mengindikasikan bahwasanya film yang terbentuk adalah Fe<sub>2</sub>O<sub>3</sub> dan Fe<sub>3</sub>O<sub>4</sub>.

**Keywords:** Baja Karbon, Air laut, SEM-EDS, *Weight loss*, XRD.

## 1. INTRODUCTION

Carbon steel continues to be extensively used in marine and power generation industries because of its favorable mechanical properties, good weldability, and relatively low cost. Despite these advantages, carbon steel exhibits limited corrosion resistance in seawater environments owing to the presence of chloride ions, dissolved oxygen, and microorganisms. Marine corrosion is recognized as one of the most significant degradation mechanisms affecting offshore structures, cooling water systems, pipelines, and seawater intake facilities. The economic impact of corrosion in marine structures

remains substantial due to repair costs, operational interruptions, and safety concerns [1], [2].

The corrosion behavior of carbon steel in seawater is controlled by electrochemical reactions occurring at the metal-electrolyte interface. Iron dissolution takes place at anodic regions while oxygen reduction occurs at cathodic sites, resulting in the formation of various iron oxides and oxyhydroxides. Refait et al. reported that corrosion product layers formed in seawater environments strongly influence corrosion progression. Corrosion products such as hematite ( $\text{Fe}_2\text{O}_3$ ), magnetite ( $\text{Fe}_3\text{O}_4$ ), lepidocrocite ( $\gamma\text{-FeOOH}$ ), and goethite ( $\alpha\text{-FeOOH}$ ) may either enhance protection or promote localized corrosion depending on their morphology and stability [3].

Temperature is one of the most influential environmental parameters affecting corrosion kinetics. An increase in temperature generally accelerates corrosion by enhancing ionic diffusion, increasing electrochemical reaction rates, and reducing the stability of protective oxide films. Recent work by Chohan et al. demonstrated that temperature exerted the most significant influence on corrosion behavior among various seawater parameters, producing more than a 70% increase in corrosion rate within the investigated range. Elevated temperatures also promoted degradation of protective corrosion layers and resulted in increased surface damage [4].

The influence of hydrodynamic conditions has also received considerable attention. Flowing seawater continuously replenishes dissolved oxygen at the steel surface while simultaneously removing corrosion products through mechanical action. Xu et al. investigated flow-accelerated corrosion of marine carbon steel in natural seawater and reported that increased flow conditions enhanced corrosion by promoting mass transfer and disrupting protective rust layers. Furthermore, the synergistic interaction between corrosion and erosion was found to significantly accelerate material degradation under aggressive marine conditions [5].

Recent studies have highlighted the importance of corrosion-product characterization in understanding marine corrosion mechanisms. Morphological and phase analyses using SEM, EDS, and XRD have demonstrated that the composition and structure of corrosion products evolve with exposure duration, seawater chemistry, and environmental conditions. Puspazikita et al. observed that low-carbon steel exposed to artificial seawater developed corrosion products dominated by hematite and magnetite, consistent with conventional seawater corrosion mechanisms. Their findings also suggested that the protectiveness of corrosion products was highly dependent on their compactness and adherence to the steel substrate [6].

Long-term marine exposure introduces additional complexity due to biological activity, environmental fluctuations, and evolving oxide layers. Melchers et al. emphasized that marine corrosion often follows a non-linear progression because corrosion-product development alters local electrochemical conditions over time. Consequently, short-term laboratory studies remain essential for understanding the fundamental influence of temperature and flow conditions on corrosion performance before implementing large-scale predictive models [2].

Although significant progress has been made in understanding seawater corrosion, knowledge gaps remain regarding the combined effects of temperature and hydrodynamic conditions on carbon steel used in motor-driven filter pipelines. Most previous investigations focused on either temperature effects or flow effects individually, whereas practical seawater systems commonly experience both simultaneously. Moreover, studies correlating weight-loss measurements with corrosion-product morphology and phase

identification are still relatively limited. Therefore, the present study aims to evaluate the corrosion behavior of carbon steel obtained from a failed motor-driven filter pipeline under static and dynamic seawater conditions over a range of temperatures using weight-loss testing, SEM-EDS analysis, and XRD characterization.

## 2. METHODOLOGY

The specimens were prepared from the failed pipeline. The specimen dimensions were 20mm length, 20mm width and thickness of 10mm. Prior to be used for experiments, the prepared specimens were treated using pickling method according to ASTM G1-90 [7]. The pickled specimens were then cleaned and washed using distilled water, acetone and stored in vacuum desiccators. The samples were weighed for the initial weight before immersion test using analytical balance (accuracy of  $\pm 0.0001$  gr). As shown in Figure 1, Optical microscopy revealed that the microstructure consisted predominantly of ferrite and pearlite, indicating that the material is a carbon steel. The observed microstructure is typical of carbon steel commonly used in seawater piping applications.

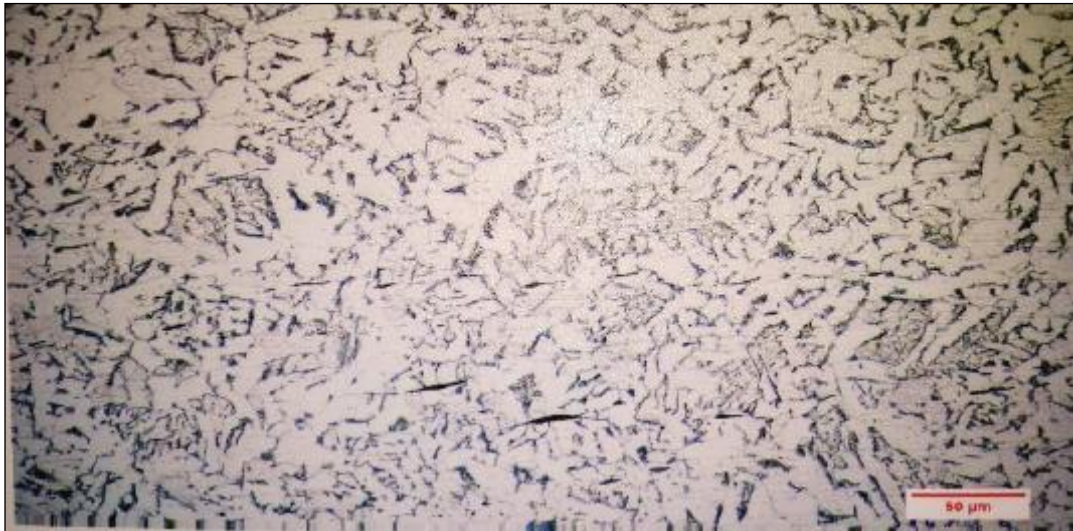


**Figure 1.** Microstructure of the sample.

The corrosion rates were studied using weight loss method as per ASTM G31-72 standard at temperature 27, 40, 60 and 80 °C [8]. Dynamic flow in this study was simulated using a magnetic stirrer operating at 2000 rpm. The test solution was treated seawater collected from a coal-fired power plant located on Java Island, Indonesia. Although detailed water chemistry data were unavailable, seawater is generally characterized by high salinity (~3.5 wt.% dissolved salts), high chloride concentration (~19,000 ppm Cl<sup>-</sup>), and relatively high electrical conductivity, which make it a highly corrosive environment for carbon steel.

The immersion time for both static and dynamic conditions were 5 days. The immersion tests were conducted in triplicate for each experimental condition. The reported corrosion rates represent the mean values of three independent measurements, while the error bars shown in the figures represent  $\pm$  one standard deviation. The corrosion testing arrangement is shown in Figure 2.

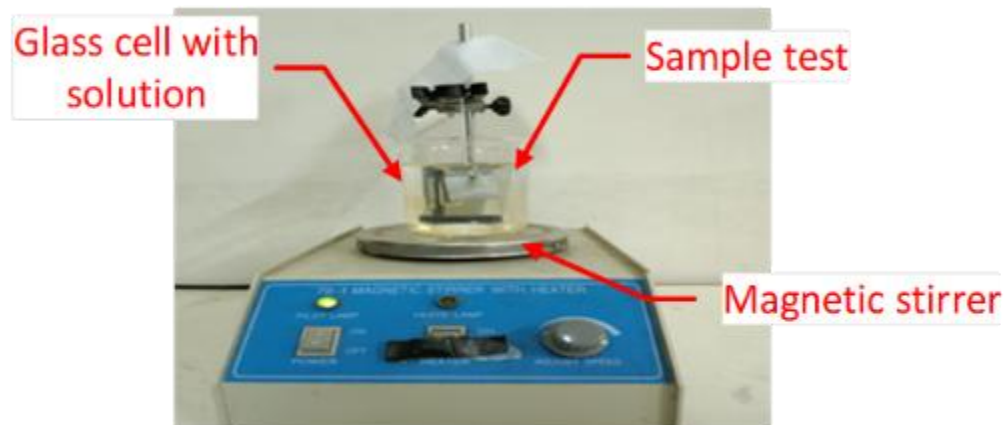


**Figure 2.** Diagram showing general arrangement of corrosion testing.

After the immersion test, the sample was cleaned with distilled water and immersed in pickling solution to remove the corrosion product. The specimen was washed with distilled water, dried in weighed to obtained the final weight. To calculate the corrosion rate, the following formula was used [9], [10].

Scanning electron microscope (Inspect, F50) attached with energy X-ray analysis (EDAX) and XRD (Shimadzu, type 6000) were used to analyse the morphology and chemical composition of the film formed.

$$CR \text{ (mmpy)} = 87.6 \times (W/D.A.T) \quad (1)$$

Where; W = weight loss in milligrams, D = metal density in  $\text{g/cm}^3$ , A = area of sample in  $\text{cm}^2$ , T = time of sample exposure in hours.

### 3. RESULTS

#### a. Corrosion rate

Corrosion rate of carbon steel in treated seawater at various temperature (27, 40, 60 and  $80^\circ\text{C}$ ) at static and dynamic conditions could be seen in Figure 3.

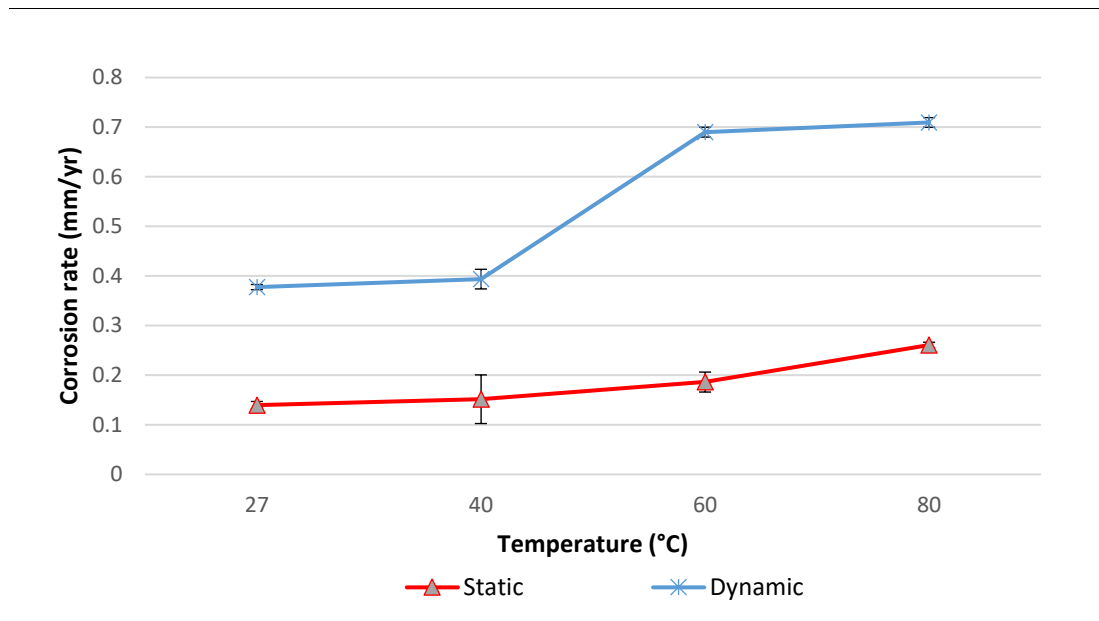


**Figure 3.** Corrosion rate of carbon steel at various temperatures (27, 40, 60 & 80°C) in static and dynamic condition. Error bars represent  $\pm$  standard deviation based on triplicate measurements ( $n = 3$ ).

From Figure 3, it is observed that the corrosion rate at temperature 27°C is 0.14 mm/yr and increases up to 98% (0.26 mm/yr) at temperature 80°C. In the dynamic conditions, no significant increasing of corrosion rate at temperature 27°C to 40°C and 60°C to 80°C. However, significant corrosion rate increment (approximately 90%) was observed when the temperature increases from 40 to 60°C.

The relatively small standard deviation values obtained from triplicate measurements indicate good experimental repeatability and confirm that the observed increase in corrosion rate with temperature is statistically consistent.

#### b. SEM (Scanning Electron Microscope)

Scanning electron microscope of carbon steel in treated seawater at temperature 27 and 80°C in static and dynamic conditions could be seen in Figure 4 to Figure 7. In static condition, at temperature 27°C, SEM showed film formation on the surface of carbon steel. It is observed that there were two layers of film formed. The first layer was characterized by spot of oval film with distinctive cleavage on its surface. While the second layer, was uniform film covered the steel surface. At temperature 80°C, it is seen that the characteristic of the film was changed. The first layer of the film was vanished and the second layer of the film was composed of fibrous typical film that might caused diffusion of corrosive species to the steel surface, hence increased corrosion rate.

In dynamic condition, at temperature 27°C, the cleavage of the film is observed and more apparent in temperature 80°C, thus increasing corrosion rate. EDS results showed the element of Fe, C and O on the film formation at both temperature (27 and 80°C) in static and dynamic condition.

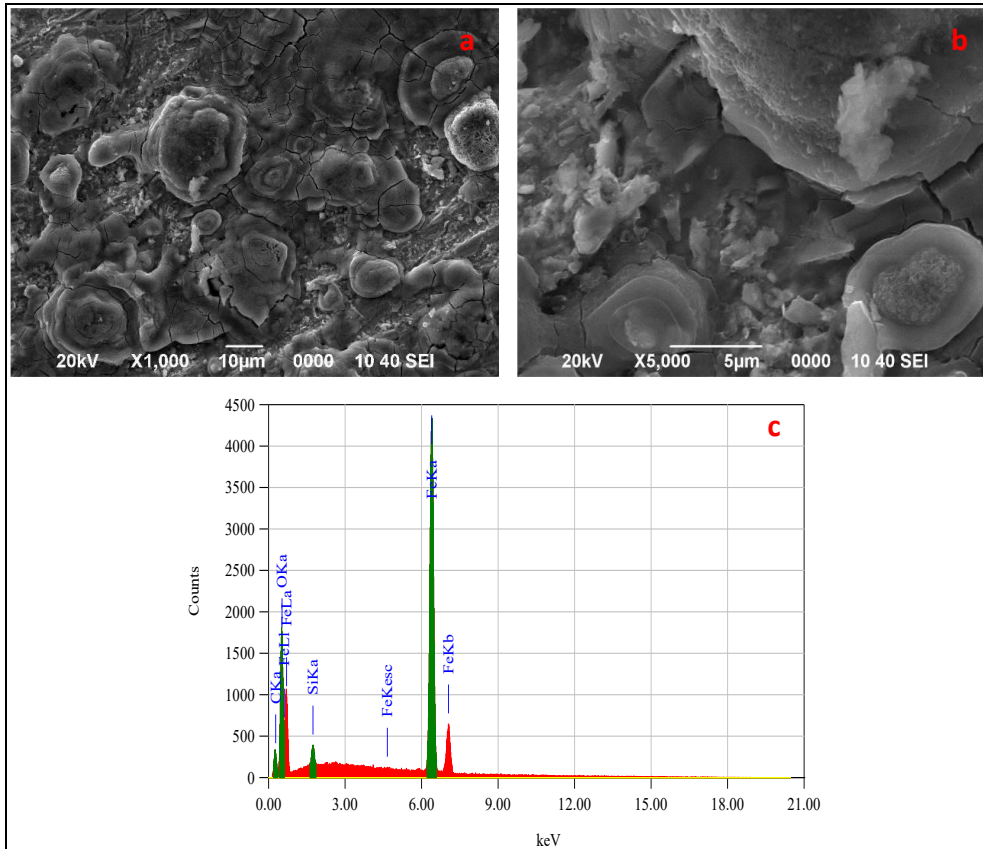


**Figure 4.** Scanning electron microscope of carbon steel in treated seawater at temperature 27°C in static condition: (a) 1000 X magnification (b) 5000 X magnification (c) EDS results.

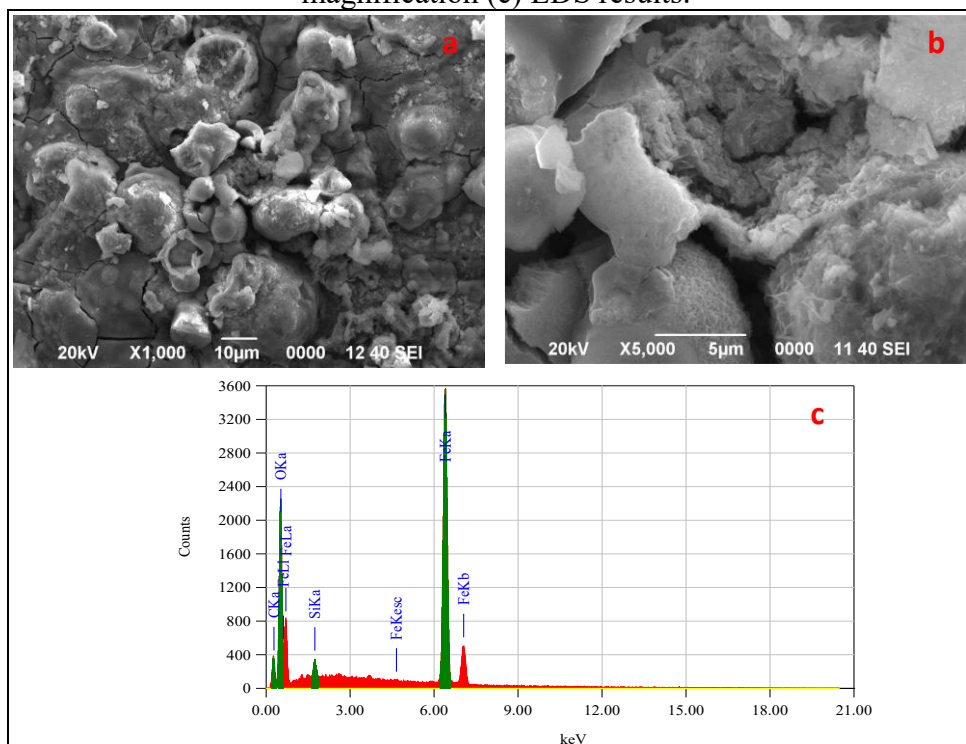


**Figure 5.** Scanning electron microscope of carbon steel in treated seawater at temperature 80°C in static condition: (a) 1000 X magnification (b) 5000 X magnification (c) EDS results.

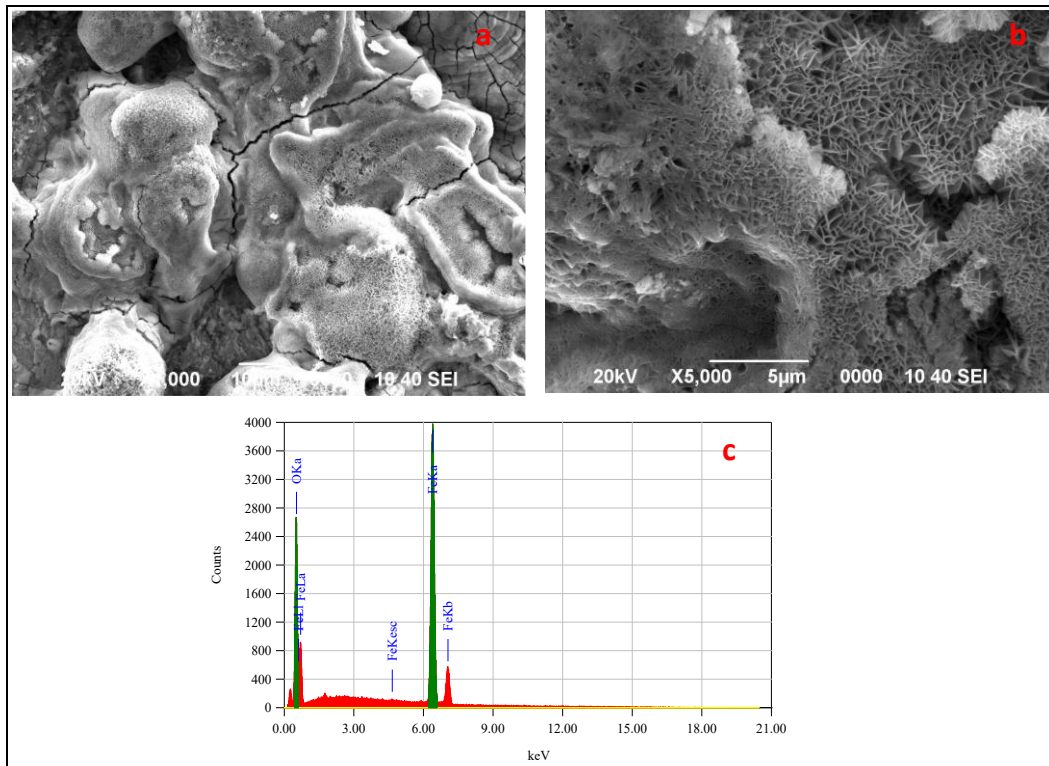


**Figure 6.** Scanning electron microscope of carbon steel in treated seawater at temperature 27°C in dynamic condition: (a) 1000 X magnification (b) 5000 X magnification (c) EDS results.



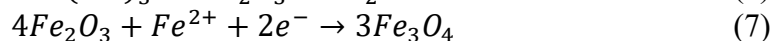
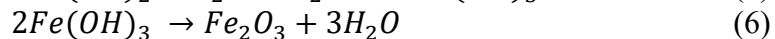
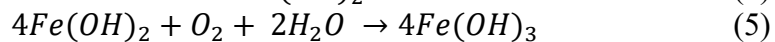
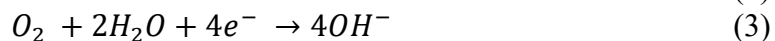
#### 4. DISCUSSION

Based on the results, the corrosion rate increased with increasing temperature under both static and dynamic conditions. Water temperature is an important factor influencing corrosion because it affects electrochemical reaction kinetics, oxygen solubility, mass transport, and biological activity [11], [12], [13], [14], [15], [16], [17], [18], [19]. The presence of chloride ions in seawater may also contribute to the breakdown of protective corrosion products. Chloride ions penetrate defects within the oxide layer and promote localized dissolution of iron, resulting in porous corrosion products and enhanced corrosion rates. This mechanism is consistent with the SEM observations showing cleavage and cracking of the corrosion product layer at elevated temperatures, particularly at 80°C.

In the dynamic condition, a significant increase of corrosion rate (approximately double) is observed at temperatures 40 - 60 °C. This behavior suggests that the corrosion process is partially controlled by mass-transfer phenomena, particularly oxygen diffusion from the bulk solution to the steel surface [17]. In addition, the results also showed that the corrosion rate in the dynamic condition is higher compared to static condition.

Higher flow velocity increases wall shear stress and fluid impact energy, thereby accelerating the removal of corrosion products and enhancing mass transfer at the metal-solution interface [13], [14]. This observation is consistent with the SEM results, which revealed cleavages and discontinuities within the corrosion-product layer. These cleavages may result from the breakdown of the corrosion-product film caused by fluid-induced shear stress.

XRD results confirmed the presence of Fe<sub>2</sub>O<sub>3</sub> (Hematite) and Fe<sub>3</sub>O<sub>4</sub> (Magnetite) as the corrosion products. The corrosion of carbon steel in aerated seawater occurs through electrochemical reactions involving anodic iron dissolution and cathodic oxygen reduction [20]. The corrosion of carbon steel in aerated seawater occurs through electrochemical reactions involving anodic iron dissolution and cathodic oxygen reduction. Ferrous ions generated at anodic sites react with hydroxyl ions to form iron hydroxides, which are subsequently converted into hematite (Fe<sub>2</sub>O<sub>3</sub>) and magnetite (Fe<sub>3</sub>O<sub>4</sub>) corrosion products. The following reactions describe the proposed corrosion mechanism [21]:



The formation of Fe<sub>2</sub>O<sub>3</sub> and Fe<sub>3</sub>O<sub>4</sub> identified by XRD is consistent with the proposed corrosion mechanism. At elevated temperatures and under dynamic conditions, the corrosion-product layer became more porous and susceptible to cracking, as observed in the SEM micrographs. Consequently, dissolved oxygen and chloride ions could more readily penetrate the corrosion layer and reach the underlying steel surface, resulting in accelerated corrosion. These observations correlate well with the increased corrosion rates obtained from the weight-loss measurements.

#### 5. LIMITATIONS OF THE STUDY

A limitation of the present work is the absence of detailed seawater chemistry data, including chloride concentration, salinity, dissolved oxygen content, and pH.

Consequently, the influence of individual seawater parameters on corrosion behavior could not be quantitatively evaluated. In addition, chemical composition analysis of the pipeline material was not available, and material identification was based primarily on metallographic examination. Future studies should incorporate comprehensive water chemistry characterization and material compositional analysis to provide a more detailed understanding of the corrosion mechanisms involved.

In addition, dynamic flow in this study was simulated using a magnetic stirrer operating at 2000 rpm. However, this method does not allow quantification of key hydrodynamic parameters such as wall shear stress, Reynolds number, or mass-transfer coefficients. The flow pattern generated by a stir bar is rotational and non-uniform, differing significantly from the fully developed turbulent flow typically present in seawater pipelines or standardized systems such as the Rotating Cylinder Electrode (RCE). Consequently, the dynamic condition used here should be interpreted as a qualitative representation of flow-accelerated corrosion rather than a precise hydrodynamic simulation. Future work incorporating RCE or controlled flow-loop systems would enable more accurate correlation between flow intensity and corrosion behavior.

## 6. CONCLUSION

Both at static and dynamic conditions, at temperature 80°C, showed a significant increasing of corrosion rate approximately two - fold higher compared to temperature 27°C. Both at static and dynamic conditions, at temperature 80°C, the film formed has porosity and cleavage so that corrosive species could diffuse to the steel surface, hence, increase corrosion rate. XRD (X-ray diffraction) showed the film formed were Fe<sub>2</sub>O<sub>3</sub> (Hematite) dan Fe<sub>3</sub>O<sub>4</sub> (Magnetite).

## 7. REFERENCES

- [1] C. Kassinis, L. Aresti, M. Koronides, P. Christodoulides, C. Michailides, and T. Onoufriou, "A review on the environment's influence on coastal marine steel corrosion and in-situ monitoring," *Journal of Materials Science: Materials in Engineering*, vol. 20, no. 1, p. 125, Oct. 2025.
- [2] R. E. Melchers, R. Jeffrey, I. A. Chaves, and R. B. Petersen, "Predicting corrosion for life estimation of ocean and coastal steel infrastructure," *Materials and Corrosion*, vol. 76, no. 6, pp. 776–789, Jun. 2025.
- [3] R. Phillippe, G. Anne-Marie, J. Marc, R. Celine, and S. Rene, "Corrosion of Carbon Steel in Marine Environments: Role of the Corrosion Product Layer," *Corrosion and Material Degradation*, vol. 1, no. 1, pp. 198–218, 2020.
- [4] I. M. Chohan, A. Ahmad, N. Sallih, N. Bheel, W. M. Salilew, and A. H. Almaliki, "Effect of seawater salinity, pH, and temperature on external corrosion behavior and microhardness of offshore oil and gas pipeline: RSM modelling and optimization," *Sci. Rep.*, vol. 14, no. 1, p. 16543, Jul. 2024.
- [5] Y. Xu *et al.*, "Flow accelerated corrosion and erosion–corrosion behavior of marine carbon steel in natural seawater," *Npj Mater. Degrad.*, vol. 5, no. 1, p. 56, Nov. 2021.
- [6] Y. M. Pusparizkita, V. A. Fardilah, C. Aslan, J. Jamari, and A. P. Bayuseno, "Understanding of low-carbon steel marine corrosion through simulation in artificial seawater," *AIMS Mater. Sci.*, vol. 10, no. 3, pp. 499–516, 2023.

- [7] “ASTM G1-90 Standard Practice for Preparing, Cleaning, and Evaluating Corrosion Test Specimens,” 1999, *ASTM*.
- [8] “ASTM G31-72 Standard Practice for Laboratory Immersion Corrosion Testing of Metals.,” 1985, *ASTM International*.
- [9] A. S. Afolabi, A. C. Muhirwa, A. S. Abdulkareem, and E. Muzenda, “Weight loss and microstructural studies of stressed mild steel in apple juice,” *International Journal of Electrochemical Science*, vol. 9, no. 11, pp. 5895–5906, 2014.
- [10] G. Priyotomo, L. Nuraini, S. Prifiharni, and S. Sundjono, “CORROSION BEHAVIOR OF MILD STEEL IN SEAWATER FROM KARANGSONG & ERETAN OF WEST JAVA REGION , INDONESIA,” *Jurnal Kelautan*, vol. 11, no. 2, pp. 184–191, 2018.
- [11] N. Otsuki, M. S. Madlangbayan, T. Nishida, T. Saito, and A. Melito, “Temperature Dependency of Chloride Induced Corrosion in Concrete,” *Journal of Advanced Concrete Technology*, vol. 7, no. February, pp. 41–50, 2009.
- [12] M. Ferry, W. B. W. Nik, and M. N. C. W, “The Influence of Seawater Velocity to the Corrosion Rate and Paint Degradation at Mild Steel Plate Immersed in Sea Water,” *Applied Mechanics and Materials*, vol. 554, pp. 218–221, 2014.
- [13] Y. Xu *et al.*, “Flow accelerated corrosion and erosion – corrosion behavior of marine carbon steel in natural seawater,” *Materials Degradation*, vol. 56, pp. 1–13, 2021.
- [14] M. Sabzi, S. Dezfuli, M. Asadian, A. Tafi, and A. Mahaab, “Study of the Effect Temperature on Corrosion Behaviour of Galvanized Steel in Seawater Environment by Using Potentiodynamic Polarization and EIS Methods,” *Materials Research Express*, pp. 1–18, 2019.
- [15] A. K. Vuppu, W. P. Jepson, and U. Ohio, “The Effect of Temperature in Sweet Corrosion of Horizontal Multiphase Carbon Steel Pipelines,” in *SPE 28809*, Melbourne: Society of Petroleum Engineers, 1994, pp. 635–638.
- [16] A. A. Al Shikshak, A. A. Mansour, and A. Taher, “Effect of Flow Velocity of Sea Water on Corrosion Rate of Low Carbon Steel,” *Applied Mchanics and Materials*, vol. 799–800, pp. 232–236, 2015, doi: 10.4028/www.scientific.net/AMM.799-800.232.
- [17] N. A. A. B. D. Alameer, “THE EFFECT OF TEMPERATURE AND pH ON THE CORROSION RATE OF CARBON STEEL in 1 M NaCl,” *Iraqi Academic Scientific Journals*, 2010.
- [18] R. E. Melchers, “Effect of Temperature on the Marine Immersion Corrosion of Carbon Steels,” *Corrosion*, no. September, pp. 768–782, 2002.
- [19] J. Owen *et al.*, “An experimental and numerical investigation of CO2 corrosion in an rapid expansion pipe geometry,” *Corrosion Science*, p. 108362, 2019.
- [20] M. Cohen, “the Formation and Properties of Passive Films on Iron,” *Canadian Journal of Chemistry*, vol. 37, no. 1, pp. 286–291, 1959, doi: 10.1139/v59-037.
- [21] M. C. Fatah, D. T. Putra, and B. A. Kurniawan, “Failure investigation of high temperature cast soot blower lance tube nozzle,” *Journal of Failure Analysis and Prevention*, vol. 20, pp. 1124–1129, 2020.